into the effect of surface oxygen protonation on the photodynamic processes of semiconductor metal oxides. All the data reveal that the electronic and structural perturbations of the polyoxometalate complex induced by solvent, including the presence or absence of electron donor-acceptor interactions, salt effects, ion pairing effects, and other medium effects are substantially less important on the photoredox chemistry than those induced by protonation.

Acknowledgment. We thank the National Science Foundation (Grant CHE-9022317) for support of this work.

Supplementary Material Available: Twelve figures addressing kinetics, quantum yield, electrochemical, and spectral (^{183}W NMR and UV-visible) measurements (13 pages). Ordering information is given on any current masthead page.

Polyene 2^1A_g and 1^1B_u States and the Photochemistry of Previtamin D_3

William G. Dauben,*,† Bimsara Disanayaka,† Dirk J. H. Funhoff,†,‡ Bryan E. Kohler,*,§ David E. Schilke,§ and Boli Zhou†

Contribution from the Departments of Chemistry, University of California, Berkeley, California 94720, and University of California, Riverside, California 92521-0403.
Received March 7, 1991. Revised Manuscript Received June 11, 1991

Abstract: The quantum yields of the photoproducts from previtamin D_3 were measured at different wavelengths with monochromatic irradiation. While the quantum yield for the cis-trans isomerization decreases with increasing wavelength near 303 nm, the ones for formation of the ring-closure products increase dramatically. This increase in photocyclization yield with decreasing photon energy is attributed to the involvement of both the 1B and 2A excited states of previtamin D_3. This hypothesis is supported by measurements of the previtamin D_3 fluorescence spectrum, fluorescence lifetime, wavelength dependence of the fluorescence quantum yield, and temperature dependence of fluorescence intensity. All of these data are integrated into a potential energy surface diagram that is consistent with both the photochemical and spectroscopic behavior.

1. Introduction

The photochemistry of previtamin D_3 (pre D_3) has been intensively studied over the last three decades. This has resulted in the identification of the photochemical products and the description of the overall photochemistry (Scheme I).[1] In recent years, the dependence of the observed solution photochemistry on excitation wavelength has been investigated. Because of its importance in optimizing the commercial production of vitamin D_3 via pre D_3, the photochemical conversion of provitamin D_3 (pro D_3) to pre D_3 has received special attention. It has been found that pre D_3 is formed from pro D_3 in significantly different yields at different excitation wavelengths.[2]

Later studies have shown that the wavelength-dependent production of pre D_3 comes from an intrinsic wavelength dependence in the photoreactions of pre D_3.[3-5] Havinga determined the quantum yields for photoproducts from pre D_3 at two different irradiation wavelengths (isolated by filter solutions) and found them to be significantly different.[3] During the following year, the effect of varying irradiation wavelength was examined at Berkeley with pulsed laser excitation to achieve greater wavelength resolution.[4] In these studies, quantum yields were most often calculated from photostationary concentrations. Effort was also made to extract quantum yields from the concentration versus time profiles of each component of the system.[5]

A wavelength effect in solution photochemistry can be attributed to a number of ground-state factors: secondary photoreactions by primary photoproducts, selective excitation of thermally equilibrated ground-state conformers, and excitation of ground-state complexes. However, wavelength dependence may also result from excited-state phenomena if photoreaction or other decay channels are competitive with the realization of a thermally equilibrated excited state.[6] We believe that this is the situation for pre D_3.

Scheme I. Photoreactions of Previtamin D_3

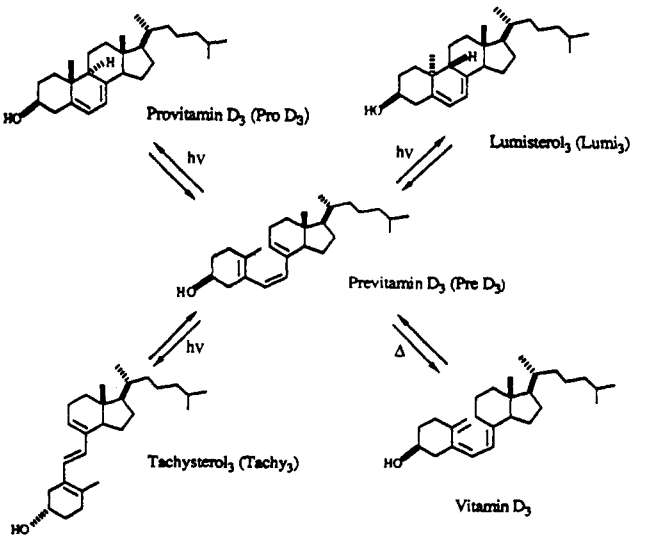

In an earlier study at Berkeley,[4] the calculated quantum yields for the formation of pro D_3 and lumisterol$_3$ (lumi$_3$) from pre D_3

† University of California, Berkeley.
‡ Recipient of a Feodor-Lynen Fellowship of the Alexander von Humboldt Foundation, 1986-1987.
§ University of California, Riverside.

(1) General reviews of the photochemistry related to the previtamin D_3 system: (a) Dauben, W. G.; McInnis, D. M. In *Rearrangements in Ground and Excited States*; de Mayo, P., Ed.; Academic Press: New York, 1980; Vol. 3, p 81. (b) Jacobs, H. J. C.; Havinga, E. In *Advances in Photochemistry*; Pitts, J. N., Jr., Hammond, G. S., Gollnick, K., Eds.; Interscience Publishers: New York, 1979; Vol. 11, p 305. (c) Norman, A. W. *Vitamin D*; Academic Press: New York, 1979.

(2) (a) Dauben, W. G.; Phillips, R. B. *J. Am. Chem. Soc.* **1982**, *104*, 355. (b) Kobayashi, T.; Yasumura, M. *J. Nutr. Sci. Vitaminol.* **1973**, *19*, 123. (c) Sato, T.; Yamachuchi, H.; Ogata, Y.; Kunii, T.; Kagei, K.; Katsui, G.; Toyoshima, S.; Yasumura, M.; Kobayashi, T. *J. Nutr. Sci. Vitaminol.* **1980**, *26*, 545. (d) Barton, D. H. R.; Hesse, R. H.; Pechet, M. M.; Rizzardo, E. *J. Am. Chem. Soc.* **1973**, *95*, 2748. (e) Pfoertner, K.; Weber, J. P. *Helv. Chim. Acta* **1972**, *55*, 921. (f) Pfoertner, K. *Helv. Chim. Acta* **1972**, *55*, 937.

0002-7863/91/1513-8367$02.50/0

doubled within the narrow wavelength range of 303–305 nm. This 2-fold increase in the quantum yields could not be attributed to a change in the absorbance of the s-cis,s-cis conformers, which are assumed to be the conformers undergoing the ring closure. Such a conformational argument would require a doubling of the absorbance of the all-cis conformers relative to the other species, which seems most improbable, given that the molar extinction coefficient of pre D_3 itself is decreased by 29% in the same wavelength range. Thus, it was suggested that the 2-fold increase was due to an excited-state effect of unknown origin.

With the knowledge that conjugated trienes have two close-lying excited states,[7] a two-state model was proposed to account for the wavelength effect in the photochemical conversion of pre D_3 to pro D_3 and lumi$_3$.[8] In this model, it was assumed that wavelengths shorter than 303 nm produced the second excited singlet state (S_2) which could decay to either the lower lying first excited singlet state (S_1) or the ground state (S_0). From S_1, the molecules could either undergo photochemical ring closure and other processes or decay to the ground state. At wavelengths longer than 303 nm, S_1 could be directly populated and energy-wasting relaxation processes of the S_2 state avoided enhancing the photochemical channels. However, preliminary investigations of pre D_3 fluorescence were interpreted as evidence against the two-state model.

The photochemical ring closure of pre D_3 is a classic six-π-electron electrocyclic reaction, which can be carried out thermally or photochemically.[1a,9,10] Although a great deal of information, both theoretical and experimental, has been accumulated with respect to the thermal reaction, much less is known about the photochemical channel. Relatively little is known about the equilibrium geometries, energies, and relaxation dynamics of the excited states involved even though this information is fundamental to understanding the observed photochemistry. To date, the potential energy surfaces that govern these processes have received little attention.

Our review of the literature led us to the conclusion that to understand more fully the wavelength dependence of the ring closure of pre D_3, three studies needed to be undertaken: (1) direct measurement of the quantum yields for the photoproducts from pre D_3 at well-defined and closely spaced wavelengths, (2) extension of the spectroscopic studies of pre D_3 to provide more detailed information on the properties of pre D_3 excited states, and (3) development of a simple picture of the potential energy surfaces involved that would coherently account for both the photochemical and spectroscopic behaviors.

We now wish to report our results for the direct measurement with high-resolution sources of the quantum yields for pre D_3 photochemistry, our determination of the spectroscopic and photophysical properties of pre D_3, and our explanation of these photochemical and spectroscopic behaviors in terms of properties of the relevant potential energy surfaces.

2. Experiments and Results

2.1. Photochemical Quantum Yields. Unless otherwise stated, all solvents used were of spectroscopic grade. Diethyl ether was distilled from sodium; reagent grade phenylacetonitrile was used as received. Previtamin D_3 was prepared by the previously published irradiation procedure[2a] and purified with an HPLC apparatus equipped with a RI detector and a Whatman M-9 10/5 10μ Particil column using 16% ethyl acetate in hexane as solvent. In order to avoid vitamin D_3 contamination, the HPLC-purified material was collected in an ice-cooled flask. Most of the eluting solvent was removed by using a rotary evaporator at 0 °C and the residue removed with a vacuum system at the same temperature. The resulting sample was sealed under vacuum and stored at −78 °C.

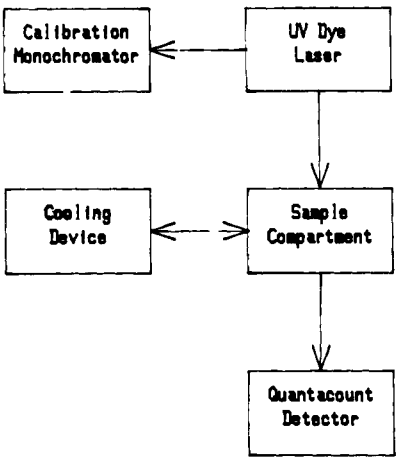

Figure 1. Apparatus configuration for measuring photochemical quantum yields.

The need for a narrow-band tunable excitation source with reasonable intensity and a sensitive and convenient method for determining the number of absorbed photons makes the execution of the quantum yield measurements a challenging task. Our experiments utilized a pulsed UV dye laser and an AMKO Quantacount. The successful application of this setup adds another dimension to quantitative organic photochemistry.

The quantum yield measurements were made with the apparatus configuration shown in Figure 1. Sample solutions of previtamin D_3 (approximately 2×10^{-3} M) in a 1 cm path length Ultrasil UV cell maintained at 0 °C were degassed by bubbling nitrogen through them for 5–10 min and then placed in the sample compartment, which was flushed with nitrogen. The samples were maintained at 0 °C in a cell holder cooled by a Lauda Kryomat. A PTI AMKO Quantacount, calibrated prior to the experiments by potassium ferrioxalate actinometry,[11] registered the number of photons absorbed by the samples. The irradiation source was a Chromatix CMX-4 pulsed UV dye laser. The laser dyes were Rhodamine 6G in methanol (280–298 nm), Rhodamine 6G in 1/1 methanol and water (295–308 nm), and Kiton Red in Ammonyx and water (310–325 nm). The Chromatrix laser wavelength readout was calibrated against a Hewlett-Packard 8450A diode array spectrophotometer. The laser bandwidth was 0.3 nm. Under the conditions of these experiments (a maximum intensity of 0.9 $\times 10^{18}$ photons cm^{-2} s^{-1} at the peak of the 10^{-6} s duration pulse), the average time between absorption events for a single molecule was always at least a factor of 10 longer than the pulse duration and several orders of magnitude longer than the excited-state decay time.

After irradiation, an aliquot of the sample solution was mixed with a volume of phenylacetonitrile standard solution and the resulting solution analyzed by HPLC. The analysis used a Rad-Pak column (10-μm silica, 10 × 0.5 cm) in a RCM-100 compression module connected to a Perkin-Elmer Series 400 pump system using 0.35% 1-pentanol in hexane as solvent: an LCD/Milton Roy 3000 spectromonitor was used to monitor the absorbance of the eluent. The statistical error was shown to be ±10%, and the calibrations of the Quantacount apparatus in

(3) Jacobs, H. J. C.; Gielen, J. W. H.; Havinga, E. *Tetrahedron Lett.* **1980**, *21*, 4013.
(4) Dauben, W. G.; Phillips, R. B. *J. Am. Chem. Soc.* **1982**, *104*, 5781.
(5) Gliesing, S.; Reichenbacher, M.; Ilge, H.-D.; Fassler, D. *Z. Chem.* **1989**, *29*, 21.
(6) Review of wavelength effects on organic photochemistry in solution: Turro, N. J.; Ramamurthy, V.; Cherry, W.; Farneth, W. *Chem. Rev.* **1978**, *78*, 125.
(7) General review: Hudson, B.; Kohler, B. E.; Schulten, K. In *Excited States*; Liu, E. C., Ed.; Academic Press: New York, 1982; Vol. 6, p 1.
(8) Dauben, W. G.; Share, P. E.; Ollmann, R. R., Jr. *J. Am. Chem. Soc.* **1988**, *110*, 2548.
(9) (a) Scherer, K. V., Jr. *J. Am. Chem. Soc.* **1968**, *90*, 7352. (b) Saltiel, J.; Lim, L.-S. N. *J. Am. Chem. Soc.* **1969**, *91*, 5404.
(10) (a) Gajewski, J. J. *Hydrocarbon Thermal Isomerization*; Academic Press: New York, 1981. (b) Marvel, E. N. *Thermal Electrocyclic Reactions*; Academic Press: New York, 1980. (c) Jutz, J. C. *Top Curr. Chem.* **1978**, *73*, 125. (d) Gilchrist, T. L.; Storr, R. C. *Organic Reactions and Orbital Symmetry*; Cambridge University Press: New York, 1972; Vol. 48.
(11) (a) Parker, C. A.; Hatchard, C. G. *Prog. R. Soc. London* **1956**, *A235*, 218. (b) Kurien, K. C. *J. Chem. Soc. B* **1971**, 218. (c) Demas, J. N.; Bowman, W. D. *J. Phys. Chem.* **1976**, *80*, 2434.

Table I. Quantum Yields of Lumisterol$_3$, Provitamin D_3, and Tachysterol$_3$ from Previtamin D_3 in Ether

wavelength, nm	lumi$_3$	pro D_3	tachy$_3$
280			
285	0.05	0.01	0.42
287	0.05	0.02	0.42
289	0.05	0.02	0.42
290			
291	0.05	0.02	0.41
292			
293	0.05	0.02	0.41
294			
295	0.05	0.02	0.41
296	0.05	0.02	0.41
298	0.06	0.02	0.40
300	0.06	0.02	0.37
301			
302	0.07	0.02	0.31
303			
304	0.13	0.03	0.28
305			
306	0.14	0.04	0.27
307			
308	0.15	0.04	0.26
309			
310			
312			
313	0.16	0.05	0.23
315	0.17	0.05	0.22
318	0.18	0.06	0.20
320	0.19	0.07	0.20
323	0.20	0.07	0.17
325	0.21	0.08	0.15
330			

quanta/count were shown to be constant in the wavelength range 250–330 nm. In the HPLC analysis, corrections were made for the absorbances of all reaction components at 271 nm using the following extinction coefficients in L mol^{-1} cm^{-1} for the standard benzyl cyanide and the four products: benzyl cyanide, ϵ = 15; pre D_3, ϵ = 1650; lumi$_3$, ϵ = 1930; vitamin D_3, ϵ = 3840; tachy$_3$, ϵ = 3580; pro D_3, ϵ = 1880. To obtain the rate of conversion at wavelengths where photoproducts also absorbed, correction was made for the number of photons absorbed by these species. This was done by using the concentrations as measured by HPLC and, following the standard procedure, calculating the actual photon absorption of pre D_3 at each excitation wavelength. The conversion on all runs was less than 5%.

The quantum yields measured in ether are listed in Table I and plotted against irradiation wavelength in Figures 2 and 3. The photoreactions of pre D_3 clearly depend on the irradiation wavelength. The cis–trans isomerization of the central double bond to tachysterol$_3$ (tachy$_3$) is more efficient at shorter wavelengths than at longer wavelengths while the reverse holds for the ring closure to pro D_3 and lumi$_3$. A sudden increase in the efficiency of the ring closure and decrease in the efficiency of isomerization occurs between 302 and 305 nm. The understanding of these changes is one of the primary goals of this paper.

2.2. Spectroscopic Measurements. Concentrated solutions of previtamin D_3 in a 1/1 by volume mixture of Decalin (44/56 cis/trans, anhydrous, Aldrich 99+%) and methylcyclohexane (Aldrich, 99% spectrophotometric grade), henceforth referred to as DMC, were prepared at Berkeley, packed in dry ice, and flown to Riverside. Immediately after arrival in Riverside, these source solutions were stored in the dark under liquid nitrogen. As needed, less concentrated stock solutions (1–2 OD cm^{-1} at 260 nm) for the spectroscopic experiments were prepared from the source solutions by diluting an aliquot of the source solution with DMC that had been purified by passage through an $AgNO_3$-impregnated alumina column.[12] As was the case for the source solutions, these solutions were stored in the dark under liquid nitrogen when they were not in use.

(12) Murray, E. C.; Keller, R. N. *J. Org. Chem.* **1969**, *34*, 2234.

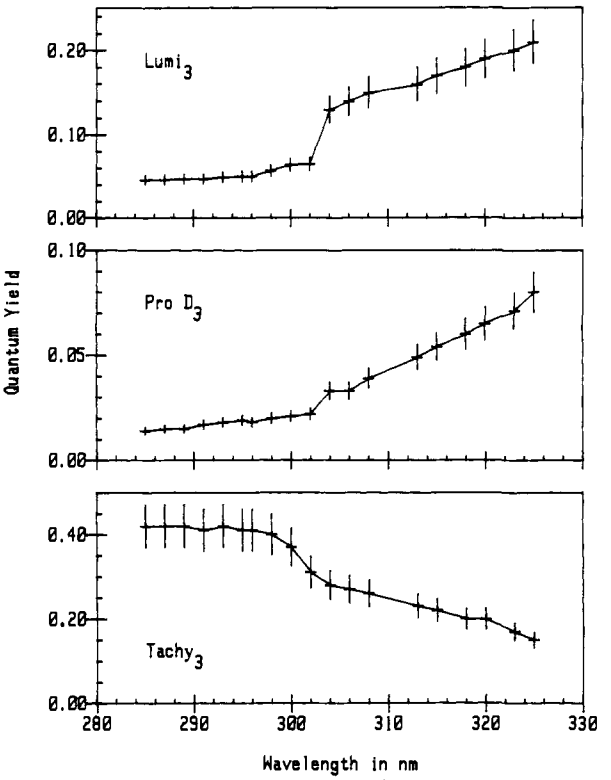

Figure 2. Quantum yields for the formation of lumisterol$_3$ (top panel), provitamin D_3 (middle panel), and tachysterol$_3$ (bottom panel) from previtamin D_3 in 0 °C ether solution versus irradiation wavelength.

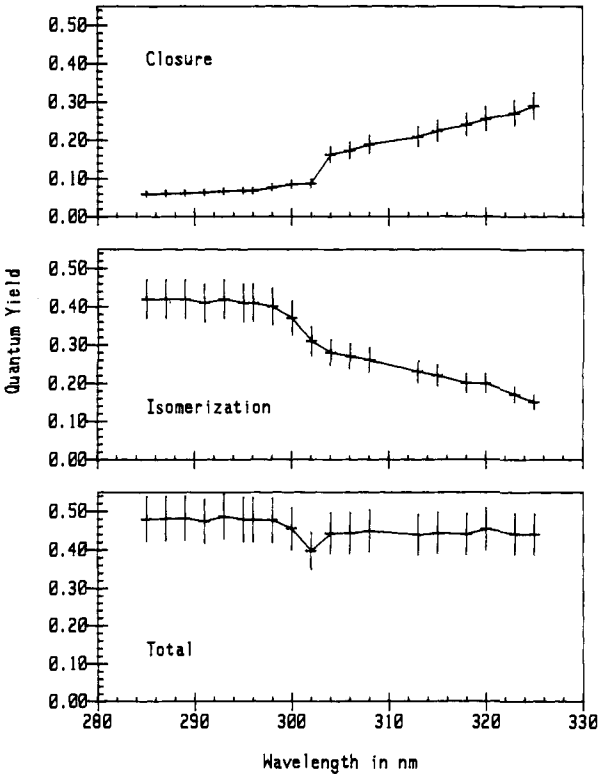

Figure 3. Quantum yields for ring closure (sum of yields for the formation of provitamin D_3 and lumisterol$_3$, top panel) and isomerization (yield for formation of tachysterol$_3$, middle pannel) and total photochemical yield (sum of the yields for making provitamin D_3, lumisterol$_3$, and tachysterol$_3$, bottom panel) from previtamin D_3 in 0 °C ether solution versus wavelength.

Before a given experiment was run, the appropriate stock solution was warmed to room temperature in the dark and then under safelights (no light with wavelengths shorter than 500 nm) approximately 1 mL was transferred to a quartz cuvette (1-mm

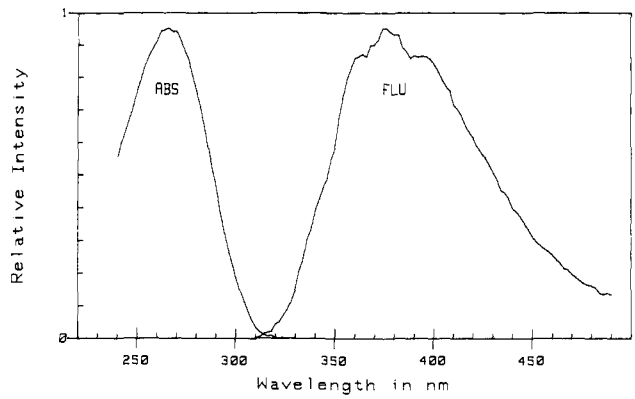

Figure 4. Low-temperature absorption (77 K) and fluorescence (4.2 K, excitation at 290 nm) spectra for previtamin D_3 in decalin/methylcyclohexane glass.

optical path length). In the emission experiments, the total absorbance at the wavelength for maximum absorbance was kept below 0.1. For the lifetime measurements, all samples were degassed and sealed on a vacuum line. For convenience, most of the spectroscopic experiments were carried out on unsealed, nondegassed samples, since it was found that the low-temperature spectroscopy of pre D_3 was not changed by degassing.

Spectra were measured under three different conditions: at 77 K with the sample cell immersed in liquid nitrogen, at 4.2 K with the sample immersed in liquid helium, and at variable temperatures (10–300 K) with the sample in a closed-cycle helium refrigerator (CTI Model 20) that was modified to allow an atmosphere of helium gas to surround the sample and the final stage of the cold head. In the variable-temperature experiments, temperature was measured at the final stage of the cold head by a calibrated diode, which was the sensor for a Lake Shore Cryotonics DRC-80C temperature controller. Absorption spectra for solutions at 77 K were measured on a Varian DMS 100S spectrophotometer. The 77 K and variable-temperature fluorescence and fluorescence excitation spectra were measured on a SPEX 212 Fluorolog 2 spectrofluorimeter by using protocols that have been described elsewhere.[13] Equipment and procedures for the 4.2 K fluorescence and fluorescence excitation spectra are also fully described elsewhere.[13] In all cases, the measured fluorescence intensity was normalized to the intensity (quanta cm^{-2} s^{-1}) of the excitation source.

Figure 4 summarizes the low-temperature absorption and fluorescence spectra seen for pre D_3 in DMC. The absorption spectrum is compared to the fluorescence excitation spectrum in the upper panel of Figure 5. We were disappointed to find that cooling to 4.2 K did not significantly increase the vibronic resolution in any of the spectra. As discussed further below, this lack of vibronic structure is due to a combination of homogeneous and inhomogeneous effects.

The fluorescence excitation spectrum (fluorescence monitored at 384 nm) shown in Figure 5 differs qualitatively from the absorption spectrum. While the fluorescence quantum yield clearly depends on the wavelength of the exciting light (lower panel, Figure 5), the fluorescence spectrum was found to have the same profile for all excitation wavelengths.

The fluorescence quantum yield of pre D_3 depends on temperature as well as excitation wavelength. Figure 6 summarizes fluorescence intensity ($\int$(photons emitted) $d\nu$/(photons absorbed), excitation at 290 nm) as a function of temperature.

2.3. Fluorescence Dynamics. Fluorescence decay kinetics were determined by using time-correlated single-photon-counting techniques. Excitation utilized second-harmonic light from a home-built jet-stream dye laser synchronously pumped by a mode-locked Ar^+ laser (Coherent Innova 200-ML), which produced pulses a few picoseconds in duration at a repetition rate

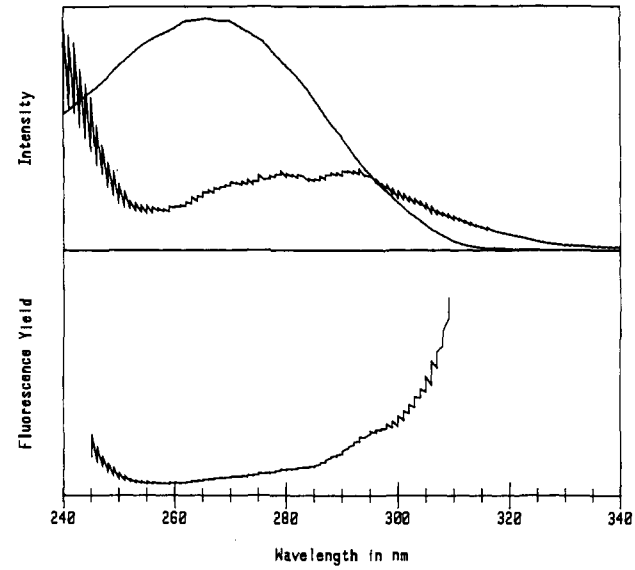

Figure 5. Upper panel: comparison of the absorption spectrum (smooth curve) and fluorescence excitation spectrum (zigzag curve, fluorescence monitored at 384 nm) measured for 77 K solutions of previtamin D_3 in decalin/methylcyclohexane glass. The maximum absorbance of the sample used to obtain the fluorescence excitation spectrum was less than 0.1. Lower panel: relative fluorescence quantum yield versus wavelength (fluorescence excitation intensity detected at 384 nm divided by absorbance) for a 77 K solution of previtamin D_3 in Decalin/methylcyclohexane glass.

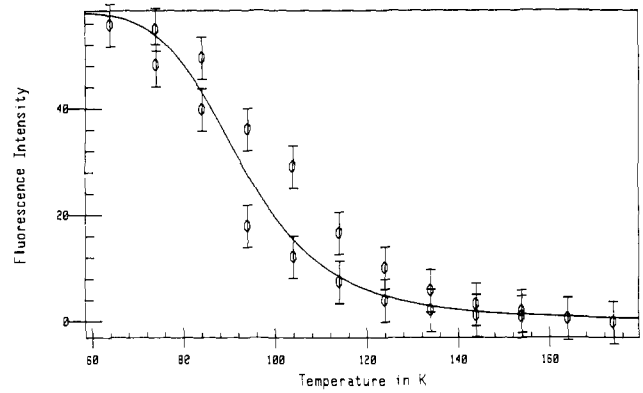

Figure 6. Integrated fluorescence intensity versus temperature for previtamin D_3 in decalin/methylcyclohexane glass. The fluorescence spectra were normalized to the intensity of the 290-nm excitation source. The solid line is the best fit curve for a thermally activated decay.

of 37 MHz. Emission from the sample was focused into a 0.25-m monochromator (Jarrell-Ash 82-410), and the light passed by the monochromator was detected by a fast-rise-time photomultiplier tube (Hamamatsu R2055) in a cooled housing (Products for Research TE104RF). The amplified photomultiplier output was sent to an Elscint STD-N-1 snap-off timing discriminator that output standardized pulses through an Epic Model 51 pulse-delay box to the start input of a time-to-amplitude converter (Tennelec TC862). The stop pulse for the time-to-amplitude converter was generated by sampling a fraction of the excitation beam with a photodiode (Hamamatsu R617U). A pulse height analyzer (Tracor-Northern TN-1705) accumulated the histogram of start to stop times that under the conditions of our experiment (less than 0.001 emitted photon per excited pulse) is equivalent to a record of fluorescence intensity versus time[14] and then transferred this histogram to a computer (Hewlett Packard 310) for processing. The time base was calibrated against the mode-locked-laser repetition rate, which was determined with a frequency counter (Hewlett Packard 5340A). Lifetimes were determined

(13) Kohler, B. E.; Spangler, C. W.; Westerfield, C. *J. Chem. Phys.* **1991**, *94*, 908.

(14) O'Connor, D. V.; Phillips, D. *Time Correlated Single Photon Counting*; Academic Press: Orlando, FL, 1984.

by least-squares fitting the measured histogram by the convolution of the histogram determined from scattered excitation light with an exponential decay. In this fitting procedure, the parameters that were varied were an overall scale factor, the lifetime, and the baseline levels for both histograms.

The fluorescence lifetime for DMC solutions of pre D_3 (excitation at 306 nm, detection at 360 nm) determined at 16 K was 2.0 ± 0.1 ns. The measured lifetime did not change with either excitation or emission wavelength.

3. Discussion

As pointed out before,[4,8] a dramatic change of photochemical quantum yields within a short range of wavelengths cannot be explained by ground-state conformational arguments. On the basis of the fact that hexatriene has two close-lying excited states, a two-state model was suggested.[8] In this section, we will analyze the spectroscopic data to derive estimates for the 0–0 excitation energies for these two states in pre D_3 and then show how the wavelength dependence of the photochemical quantum yields, the wavelength dependence of the fluorescence quantum yield, and the temperature dependence of fluorescence intensity may be coherently understood within the two-state model.

3.1. State Energies. The measurement of vibrationally resolved spectra for linear polyenes has led to important advances in our picture of electronic structure in these important molecules.[7] It is now well established that the ordering of polyene excited singlet states (trienes and longer) is inverted from what would be predicted by molecular orbital theory at the Hartree–Fock level: that is, the singlet state that is derived from the ground-state configuration by promoting one electron from the highest energy occupied molecular orbital (HOMO) to the lowest energy unoccupied molecular orbital (LUMO), hereafter referred to as the 1B state, is not the lowest energy excited singlet state S_1 but the next higher singlet S_2. S_1 is a state that, because of electron correlation, is necessarily described as a configurational mixture in which the configuration where two electrons are excited from the HOMO to the LUMO is key. In the following, we shall refer to this state as 2A and freely use the associations S_1 = 2A and S_2 = 1B.

We have recently presented a simple model for polyene electronic structure that accurately reproduces all of the 0–0 excitation energies for the 2A and 1B states that have been measured for all-trans polyenes in low-temperature hydrocarbon solutions (three through eight double bonds in conjugation).[15] The 2A and 1B 0–0 excitation energies for unsubstituted hexatriene calculated by using this model are 34 260 cm^{-1} (292 nm) and 37 740 (265 nm), respectively. Although the excitation energy for the 2A state of hexatriene in hydrocarbon solution has not yet been directly measured, the 0–0 excitation energy for gas-phase *cis*-hexatriene is 34 393 cm^{-1} (292 nm).[16] A close agreement between the extrapolated 0–0 excitation energy in hydrocarbon solution and that measured for the isolated molecule is expected, since studies on octatetraene have established that polyene 2A excitation energies are nearly identical for cis and trans isomers[17] and do not change significantly with solvent polarizability.[18] For the longer polyenes, α,ω-dialkyl substitution shifts polyene 2A and 1B excitation energies slightly to lower values. In contrast, for low-temperature hydrocarbon solutions of an α,ω-dialkylhexatriene, the simple model gives 2A and 1B 0–0 excitation energies of 35 650 cm^{-1} (281 nm) and 36 050 cm^{-1} (277 nm), respectively, which would imply that in the triene alkyl substitution shifts the 2A state to higher energy. A solid conclusion on this point must await further experiments. In addition to being alkyl substituted, the triene chromophore in pre D_3 contains s-cis linkages that are known to shift polyene 1B excitation energies to lower energy (2920 cm^{-1} for butadiene,[19] 1750 cm^{-1} for octatetraene[20]). If the shift for the triene were intermediate between these values (2335 cm^{-1}), then the 1B 0–0 excitation energy for pre D_3 would be expected to be approximately 36 050 cm^{-1} − 2335 cm^{-1} = 33 715 cm^{-1} (297 nm). The 2A 0–0 excitation energy expected for pre D_3 is much less certain. For gas-phase *cis*-hexatriene, the 2A 0–0 excitation energy is 5270 cm^{-1} lower than the 1B 0–0 excitation energy.[16] In hydrocarbon solutions, this gap is expected to be reduced to 3480 cm^{-1} (difference between the 1B 0–0 excitation energy measured in hydrocarbon solution and the 2A 0–0 excitation energy measured in the gas phase). The extrapolations of 0–0 excitation energies for dialkyl-substituted polyenes predicts a gap of only 400 cm^{-1},[15] but we believe that, since the effects of alkyl substitution are small and nearly the same for the 2A and 1B states, the 3850-cm^{-1} gap determined from the directly measured excitation energies is the better estimate. With little direct information on the effect of the s-cis linkages on the 2A excitation energy (for octatetraene they induce a 1200-cm^{-1} red shift[20]), all that can be said a priori is that the 2A 0–0 excitation energy for pre D_3 is expected to be less than, but possibly near, that of the 1B state.

When it is possible to measure vibrationally resolved absorption and emission spectra, the 0–0 excitation energies for the 2A and 1B states of a given linear polyene are easily and unambiguously determined. Presumably because of the complexity of the solute, the optical spectra for pre D_3 that we have measured are inhomogeneously broadened to the point that individual vibronic bands are not resolved (Figure 4). Nonetheless, even in this case, we can demonstrate that the strong absorption and the fluorescence involve different excited states: that S_1 from which the fluorescence originates is the polyene 2A state and that the polyene 1B state that is responsible for the strong absorption is S_2. This conclusion follows from a Franck–Condon analysis of the absorption and emission profiles and a comparison of the excited-state lifetime calculated from the measured absorption intensity to that determined from the fluorescence decay time and quantum yield.

3.1.1. Franck–Condon Analysis. For an electronically allowed transition like the polyene 1A to 1B absorption, the intensity of a given vibronic band is proportional to a Franck–Condon factor—the square of the $(3N - 6)$-dimensional overlap integral between ground- and excited-state vibrational wave functions. If the vibrational states can be adequately described in terms of separable harmonic modes, recursion relations make the computation of these Franck–Condon factors extremely straightforward.[21] Previous studies have shown that the vibronic profiles of the linear polyene 1A to 1B transition are accurately reproduced when it is assumed that only two normal modes, the C—C and C=C symmetric stretches, are involved in the vibronic development and that, of these, the C=C symmetric stretch is by far the most important.[22] This is also true for some steroids.[23] This and the fact that inhomogeneous line profiles as well as low-frequency vibronic progressions are reasonably modeled by Gaussians make it reasonable to assume that the broad envelope of the 1A → 1B transition of any linear polyene should be well fit by the superposition of Gaussians whose relative intensities are given by the Franck–Condon factors calculated for a single C=C stretching mode. In the case of pre D_3, this expectation is met only if the absorption and fluorescence spectra are allowed to have different 0–0 energies.

The Franck–Condon analysis of the absorption and fluorescence spectra of pre D_3 used experimentally determined C=C symmetric stretch frequencies in the 1A (1622 cm^{-1}),[24] 2A (1724 cm^{-1}),[16]

(15) Kohler, B. E. *J. Chem. Phys.* **1990**, *93*, 5838.
(16) (a) Buma, W. J.; Kohler, B. E.; Song, K. *J. Chem. Phys.* **1990**, *92*, 4622. (b) Buma, W. J.; Kohler, B. E.; Song, K. *J. Chem. Phys*, in press.
(17) Kohler, B. E.; Spiglanin, T. A. *J. Chem. Phys.* **1984**, *80*, 3091.
(18) Kohler, B. E. In *Conjugated Polymers: The Novel Science and Technology of Conducting and Nonlinear Optically Active Materials*; Bredas, J. L., Silbey, R., Eds.; Kluwer Press: Dodrecht, The Netherlands, 1991.
(19) Squillacote, M. E.; Sheridan, R. S.; Chapman, O. L.; Anet, F. A. *J. Am. Chem. Soc.* **1979**, *101*, 3657.
(20) Ackerman, J. R.; Forman, S. A.; Hossain, M.; Kohler, B. E. *J. Chem. Phys.* **1984**, *80*, 39.
(21) Manneback, C. *Physica* **1951**, *17*, 1001.
(22) (a) Granville, M. F.; Kohler, B. E.; Snow, J. B. *J. Chem. Phys.* **1981**, *75*, 3765. (b) Kohler, B. E.; Spiglanin, T. A.; Hemley, R. J.; Karplus, M. *J. Chem. Phys.* **1984**, *80*, 23.
(23) (a) Andrews, J. R.; Hudson, B. S. *Chem. Phys. Lett.* **1979**, *60*, 380. (b) Pierce, B. M.; Bennett, J. A.; Birge, R. R. *J. Chem. Phys.* **1982**, *77*, 6343.
(24) Langkilde, F. W.; Willbrandt, R.; Nielsen, O. F.; Christensen, D. H.; Nicolaisen, F. M. *Spectrochim. Acta, Part A* **1987**, *43*, 1209.

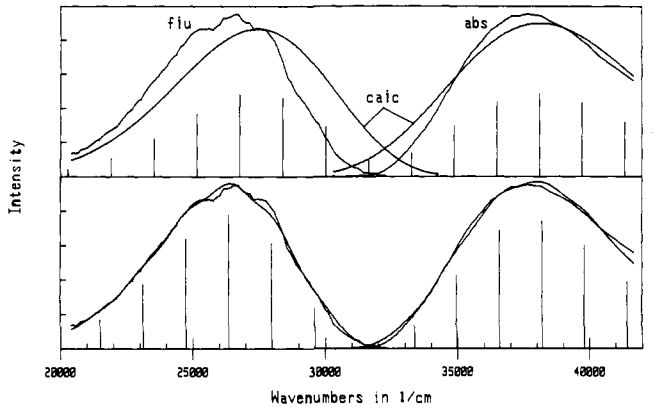

Figure 7. Single-mode Franck–Condon fits to absorption and fluorescence spectra assuming that a single excited electronic state is involved (upper panel) and that absorption and fluorescence involve different excited states (lower panel). The vertical lines show the calculated spectrum before convolution with the Gaussian function. In the upper panel, the measured absorption and fluorescence spectra are labeled abs and flu, respectively, and the calculated spectra are labeled calc. In the lower panel, the measured and calculated spectra are almost indistinguishable.

and 1B (1618 cm^{-1})[25] states. Figure 7 compares the measured spectra to those calculated by assuming that a single excited state is involved (upper panel) and assuming that the absorption and emission spectra have different origins (lower panel). Clearly, even though there is nonzero overlap between the absorption and fluorescence spectra, the smallness of this overlap is inconsistent with the relatively narrow widths of the vibronic envelopes. Said differently, if a single excited state were involved, the small overlap between the absorption and fluorescence spectra would imply a large Franck–Condon displacement. A large Franck–Condon displacement would give long progressions either in the explicitly modeled C=C stretch or in the low-frequency modes subsumed in the Gaussian band shape. The spectra do not manifest these progressions.

The 1B 0–0 excitation energy of 33 350 cm^{-1} (300 nm) determined from the two-state Franck–Condon fit is close to the estimate of 37 715 cm^{-1} (297 nm) derived in section 3.1. The best fit value for the 2A 0–0 excitation energy of 29 600 cm^{-1} (338 nm) implies a 1B–2A gap of 3750 cm^{-1}, which is very close to that obtained by extrapolating excitation energies for unsubstituted polyenes (3480 cm^{-1}) but is much larger than the extrapolated gap for dialkyl-substituted polyenes (400 cm^{-1}). Because the Gaussian line shape may, at least to some extent, compensate for progressions in low-frequency modes, the 0–0 excitation energies obtained by the Franck–Condon analysis could well be shifted by at least one Gaussian σ (1165 cm^{-1} for fluorescence, 1120 cm^{-1} for absorption). Accordingly, 3750 cm^{-1} is an upper bound estimate for the 1B–2A gap of pre D_3. The decomposition of the Gaussian profile into contributions from lifetime broadening and from unresolved vibrational progressions will require experiments that have higher information content, such as fluorescence measurements on more homogeneous systems or measurement of Raman excitation profiles.

The best fit normal-coordinate displacements from the Franck–Condon fits (0.06 $cm^{1/2}$ for both the 1B and 2A states) are significantly larger than the displacements determined for other linear polyenes (for example, for octatetraene, the 1B and 2A double-bond displacements are 0.02 and 0.03 $cm^{1/2}$, respectively).[26] This is probably due to the fact that all of the Franck–Condon development has been put into a single mode.

3.1.2. Lifetime-Intensity Analysis. The relationship between absorption strength and radiative decay rate has been put into a form appropriate for molecular electronic spectra by Strickler and Berg.[27] Numerical integration of the pre D_3 absorption spectrum shown in Figure 4 and application of eq 14 from ref 27 employing the measured solvent refractive index of 1.4488 gives a predicted lifetime for radiative decay of 4.3 ns. The directly measured radiative decay time for pre D_3 in DMC at 16 K is 2.00 ns. The quantum yield for fluorescence under similar conditions is 0.18 ± 0.02,[8] which means that the lifetime for radiative decay is 11.1 ± 1.4 ns, 2.6 times longer than that predicted from the absorption intensity. This apparent discrepancy, which is always found in linear polyene spectroscopy, has been shown in all other cases to reflect the fact that the fluorescence does not come from the strongly allowed 1B state but from a lower lying, weakly absorbing 2A state. This must also be the case for pre D_3.

The 11,1-ns lifetime for radiative decay is short in comparison to the 100–200-ns decay lifetimes (reciprocal of the sum of rates for radiative and nonradiative decay) that have been measured for octatetraene in low-temperature hydrocarbon solutions.[28] This implies that, in going from the trans planar unsubstituted polyene to pre D_3, the hexatriene 2A and 1B states are significantly mixed. This mixing intensifies the extinction coefficient for absorption to the 2A state, making it possible to preferentially excite to the 2A surface at the red edge of the absorption band.

3.2. Wavelength Dependence of the Fluorescence Yield. The absorption and fluorescence excitation spectra measured for 77 K DMC solutions of pre D_3 scaled to have the same intensity at 295 nm are given in the upper panel of Figure 5. Since the fluorescence intensity at a given wavelength is proportional to the probability for absorbing a photon times the probability for emitting a photon, the fact that these spectra cannot be made identical by scaling indicates that the quantum yield for fluorescence depends strongly on excitation wavelength. The fluorescence quantum yield versus wavelength (fluorescence excitation intensity divided by absorbance) plotted in the lower panel of Figure 5 decreases strongly with decreasing wavelength in the vicinity of 300 nm, the same region where the quantum yield for ring closure drops sharply with decreasing irradiation wavelength. Since this is exactly the wavelength region for the 1B 0–0 excitation energy, both of these phenomena are consistent with the presence of a radiationless pathway from the 1B state to the ground state that efficiently competes with relaxation within the excited-state manifold. This is known to be the case for isolated diphenylbutadiene[29,30] although, in the case of diphenylbutadiene, the addition of buffer gas or solvation makes the rate of thermalization on the excited-state manifold significantly faster than that of the 1B dark channel.[30]

Because the dark channel from the pre D_3 1B state to the ground state competes with vibrational equilibration, its associated rate must be significantly faster than the rate for radiative decay from the 1B state. This is supported by the finding that the shape (intensity versus wavelength) of the fluorescence spectrum does not depend on excitation wavelength. That is, there is no evidence for emission from S_2.

3.3. Temperature Dependence of Fluorescence Intensity. If decay from the 1B state to the ground state competes with decay to the lower lying 2A state or if the 2A state has thermally activated decay channels, we expect the total fluorescence yield to depend on temperature. In the simplest formulation, the decay rate for the 2A state can be written as

$$k = k_r + k_{nr} + k_b \exp(-\Delta E/kT) \quad (1)$$

where k_r and k_{nr} are the intrinsic radiative and nonradiative decay rates of the 2A state and the exponential term describes thermally activated decay. In the regime where $k_r + k_{nr}$ does not significantly change with temperature, the overall fluorescence intensity I_f should be described by the expression

$$I_f = A/(1 + B \exp(-\Delta E/kT)) \quad (2)$$

(25) Leopold, D. G.; Pendley, R. D.; Roebber, J. L.; Hemley, R. J.; Viada, V. *J. Chem. Phys.* **1984**, *81*, 4218.
(26) Kohler, B. E. *Synth. Met.* **1991**, 41–43, 1215.
(27) Strickler, S. J.; Berg, R. A. *J. Chem. Phys.* **1962**, *37*, 817.
(28) (a) Ackerman, J. R.; Kohler, B. E.; Huppert, D.; Rentzepis, P. M. *J. Chem. Phys.* **1982**, *77*, 3967. (b) Kohler, B. E.; Snow, J. B. *J. Chem. Phys.* **1983**, *79*, 2134.
(29) Heimbrook, L. A.; Kohler, B. E.; Spiglanin, T. A. *Proc. Natl. Acad. Sci. U.S.A.* **1983**, *80*, 4580.
(30) Itoh, T.; Kohler, B. E. *J. Phys. Chem.* **1988**, *92*, 1807.

where $A = k_r/(k_r + k_{nr})$ times a scaling constant and $B = k_b/(k_r + k_{nr})$. The solid line in Figure 6 shows the best fit of eq 2 to the integral of normalized pre D_3 fluorescence intensity versus temperature (two independent runs). The best fit parameter values of interest are $B = 1.6\ (\pm 2.6) \times 10^4$, which is the ratio of the thermally activated decay rate to the 2A state decay rate, and $\Delta E = 630 \pm 120\ cm^{-1}$ (1.8 ± 0.3 kcal/mol). The measured low-temperature lifetime of the 2A state is 2 ns, which means that, in this model, the lifetime for decay to the ground state via the thermally activated channel k_b is of the order of 100 fs. If this decay goes through the 1B state, the ΔE value corresponds to the thermodynamic value for the 1B–2A gap. In all cases where a linear polyene has a significant spread in microscopic environments, the thermodynamic gap between 2A and 1B states is significantly smaller than the spectroscopic gap (energy difference between 0–0 band centers). The exponential dependence of the rates on the energy gap skews the thermodynamic value from the average value for the ensemble toward the minimum. As discussed below, it can also be that the decay goes through the 2A state and that the ΔE determined from the fit represents the barrier to ring closure on the 2A potential energy surface. This can be resolved by experiments on a simpler model system in a more homogeneous environment that are in progress.

3.4. Quantum Yields in the Two-State Model. Since the 2A state lies lower than the 1B state, at sufficiently long wavelengths it should be the only state excited. Thus, we can associate the photochemical quantum yields measured at long wavelength to 2A state quantum yields. Short-wavelength excitation will almost exclusively prepare the 1B state because of its significantly higher absorption strength. This means that the photochemical quantum yield measured for a given process for short-wavelength excitation is a sum of two terms: The 1B state quantum yield plus the product of the 2A state quantum yield times the quantum yield for the 1B state to convert to the 2A state. We arbitrarily take the 2A state quantum yields to be those measured for 325-nm excitation and the composite quantum yields to be those measured for 291-nm excitation. Also, it is assumed that there is no conformational effect on light absorption.

Given the gross simplifications that are involved in this analysis, it is sensible to add the quantum yields for $lumi_3$ and pro D_3 to get a total quantum yield for ring formation, ϕ_r. The quantum yield for $tachy_3$ is ϕ_i (i for isomerization) and the quantum yield for decay (no photochemistry) is ϕ_d. Adding a second index to designate the excited state (A or B) and designating the yield for the 1B state to relax to the 2A state as ϕ_B, we have $\phi_{Ar} = 0.29$, $\phi_{Ai} = 0.15$, $\phi_{Ad} = 0.56$, $\phi_{Br} + \phi_{BA}\phi_{Ar} = 0.06$, $\phi_{Bi} + \phi_{BA}\phi_{Ai} = 0.41$, and $\phi_{Bd} + \phi_{BA}\phi_{Ad} = 0.53$. The fact that all of the quantum yields must lie between 0 and 1 means that ϕ_{BA}, the quantum yield for the 1B state to relax to the 2A state, can be no longer than 0.21. At the lower limit, $\phi_{BA} = 0$, we obtain $\phi_{Br} = 0.064$, $\phi_{Bi} = 0.41$, and $\phi_{Bd} = 0.526$. At the upper limit, $\phi_{BA} = 0.21$, we obtain $\phi_{Br} = 0$, $\phi_{Bi} = 0.38$, and $\phi_{Bd} = 0.41$. In either case, the quantum yield for ring formation from the 1B state is nearly zero so that the decay channels intrinsic to the 1B state are isomerization, decay to the 2A state, and, necessarily, an independent competitive channel for decay to the ground state.

3.5. Potential Surfaces. The electronic states of cyclohexadiene and *cis*-hexatriene can be classified according to how they transform under the C_{2v} point group. The states that do not change sign under rotation about the C_2 axis lying in the molecular plane and bisecting the central bond are labeled A; those that do change sign are labeled B. The symmetries of the states can be derived from the symmetries of the occupied molecular orbitals by following the multiplication rule. The energy ordering of the states is indicated by a number preceding the symmetry label. For example, the ground state of cyclohexadiene or *cis*-hexatriene is 1A, the lowest excited state of A symmetry is 2A, etc.

Mathies and co-workers have reported resonance Raman studies of the ring opening of cyclohexadiene to *cis*-hexatriene.[31] They observed a fast dephasing of the initially formed 1B state of cyclohexadiene but found that the differences between the equilibrium geometries of the 1A and 1B states were very small relative to the displacements required for the ring-opening reaction. It was thus concluded that the fast decay could only be rationalized by invoking an allowed crossing of potential energy surfaces through which the 1B state could cross to a second surface that led to the product. The dipole-forbidden 2A state was proposed to be the second state. While it is likely that the 0–0 excitation energy for the 2A state is lower than that of the 1B state, the ordering has not yet been unequivocally fixed.

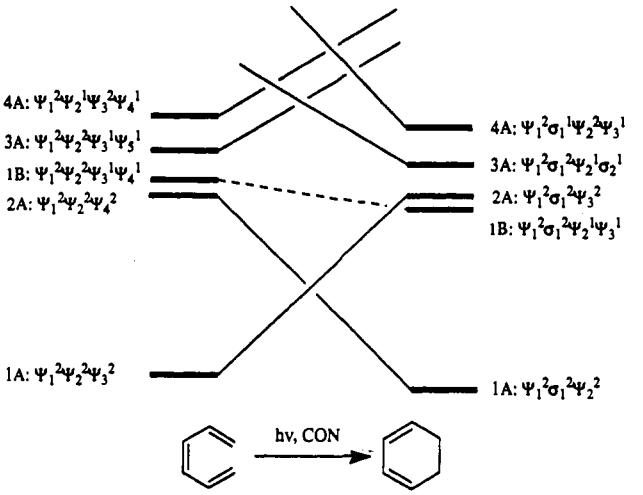

Figure 8. State correlation diagram for the photochemical conrotatory ring closure of *cis*-hexatriene.

That the 2A state is an intermediate state in this reaction was also predicted by a recent MRD CI calculation. Share et al.[32] suggested that the photochemical transformation of cyclohexadiene to *cis*-hexatriene passes through a minimum on the 2A excited-state potential energy surface that has its origin in an avoided crossing between A states. Oosterhoff[33] and Devaquet[34] suggested the same mechanism for the electrocyclic reaction of butadiene.

These experimental and theoretical results call attention to state symmetry control of the reaction.[35] Although the consequences of symmetry preservation in this case are widely known, our discussion is aided by a quick review. Under the assumption that the carbon framework of *cis*-hexatriene remains planar as the ring closes, two symmetry elements have the potential of being conserved: the C_2 axis that bisects the central bond and the mirror plane containing this axis that is perpendicular to the central bond. The molecular orbitals of reactant and product are labeled s (symmetric) or a (antisymmetric) with respect to the symmetry element that is to be observed—disrotation preserves the plane and conrotation preserves the axis. The orbitals of reactant and product are then correlated via the symmetry correlation principle[35a-c] to give an orbital correlation diagram from which a state correlation diagram can be derived (see Figure 8). The allowed photochemical reaction is conrotatory, the excited 2A state of *cis*-hexatriene correlating with the ground state of cyclohexadiene. (Although, because of the importance of electron correlation, the 2A state is necessarily a mixture of configurations, this mixture is dominated by the state derived from the ground state by promoting two electrons from the HOMO to the LUMO.) The

(31) Trulson, M. O.; Dollinger, G. D.; Mathies, R. A. *J. Chem. Phys.* **1989**, *90*, 4274.

(32) Share, P. E.; Kompa, K. L.; Peyerimhoff, S. D.; Van Hermert, M. C. *Chem. Phys.* **1988**, *120*, 411.

(33) Oosterhoff, L. J.; van der Lugt, W. Th. A. M. *J. Am. Chem. Soc.* **1969**, *91*, 6042.

(34) Grimbert, D.; Segal, G.; Devaquet, A. *J. Am. Chem. Soc.* **1975**, *97*, 6629.

(35) Turro, N. J. *Modern Molecular Photochemistry*; Benjamin/Cummings Publishing Co., Inc.: Menlo Park, CA, 1978. (b) Woodward, R. B.; Hoffmann, R. *The Conservation of Orbital Symmetry*; Academic Press: New York, 1970. (c) Lowry, T. H.; Richardson, K. S. *Mechanism and Theory in Organic Chemistry*; Harper and Row: New York, 1981. (d) Longuet-Higgins, H. C.; Abrahamson, E. W. *J. Am. Chem. Soc.* **1965**, *87*, 2046.

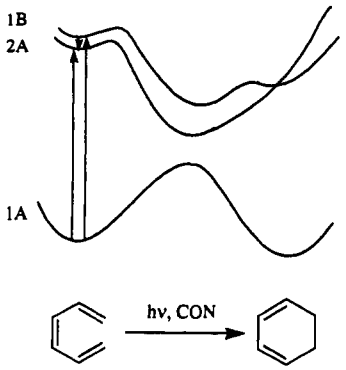

Figure 9. Potential surface diagram for the photochemical conrotatory ring closure of *cis*-hexatriene.

qualitative form of the potential energy surfaces for the ground and first excited A states along the coordinate for conrotatory closure is that of an avoided crossing. This is supported by the fact that the spectroscopic data indicate a local minimum on the 2A surface of hexatriene that is only slightly displaced relative to the minimum on the ground-state surface.[16] Although symmetry considerations predict that the 1B state of *cis*-hexatriene correlates with the same state of cyclohexatriene, they give no information on the profile. However, Franck–Condon analysis of the absorption spectrum of *trans*-hexatriene[22a] led to the conclusion that differences in the equilibrium geometries of the ground and excited 1B states were relatively small. This is supported by measurements of the absorption spectra of jet-cooled *trans*- and *cis*-hexatriene.[25] Resonance Raman studies of the 1B state of cyclohexadiene have shown that the 1B–2A crossing point is only a small fraction of the distance along the ring-opening coordinate to the equilibrium geometry of *cis*-hexatriene.[31] This fixes the starting and ending portions of the 1B state potential surface. Since there is no experimental information for the middle portion, we adopt the shape suggested by the MRD CI calculation.[32] The final result is given in Figure 9.

The form of the potential energy surface along the coordinate for conrotatory ring closure shown in Figure 9 is consistent with all that is known at this point about the photophysical and photochemical properties of dienes and trienes. The best estimate for the form of this potential energy surface along the isomerization coordinate comes from work on the low-temperature photoisomerization of octatetraene.[36-38] Two features are of special relevance to this discussion. First, with respect to isomerization, the 2A potential energy surface is extremely flat (the difference between the highest barrier and the lowest minimum is only 880 cm^{-1} or 2.6 kcal/mol). Second, at low temperatures, isomerization is adiabatic; that is, it takes place on the 2A surface leading to an excited (fluorescent) product.[38]

Since we can obtain vibrationally resolved 1A → 2A excitation spectra for *cis*-hexatriene, we know that there are barriers to all possible nuclear motions, including those associated with isomerization and ring closure. As the temperature is increased from 0 K, both isomerization and ring closure should be enhanced. However, the octatetraene studies tell us that only ring closure will deactivate the excited state. Thus, if the temperature dependence of fluorescence intensity were consistent with a thermally activated decay whose activation energy was less than the 1B–2A gap, that activation energy would reasonably be identified with ring closure on the 2A potential energy surface. We believe that this is the most plausible explanation for the observed temperature dependence of fluorescence intensity.

4. Conclusion

The large change of the photochemical quantum yields in the ring closure of pre D_3 over a 2–3-nm change in excitation wavelength is best rationalized on the basis of the participation of both the 2A and 1B excited states in the photoreaction. Qualitatively correct potential surfaces for these states along the conrotatory coordinate can be constructed from consideration of orbital symmetry concepts and of a variety of spectroscopic information. These potentials indicate that the photochemical ring closure of pre D_3 goes through a well (avoided crossing) on the 2A surface. This well is a leakage channel (a funnel) from the pre D_3 2A state to the ground state of the ring closure products, since at that point the two states have their minimum separation. Excited molecules can get into this well by two pathways. With excitation wavelengths shorter than 303 nm, we postulate that the 1B state is initially excited and subsequently partitions between isomerization, decaying to the 2A state or decaying to the ground state. Those molecules that reach the 2A state move into the well that leads to ring closure. Alternatively, for wavelengths longer than 305 nm, the 2A state is directly excited and the relaxation path from the 1B state to the ground state or isomerization in the 1B state is avoided.

The mechanistic concepts developed here can be applied to the general area of photochemical six-π-electron electrocyclic reactions.

Finally, we note that the diagram in Figure 9 could also account for the fact that there is no wavelength effect in the reverse reaction, the ring opening of pro D_3 to pre D_3.[3] If the 2A state of pro D_3 is higher in energy than the 1B state, as indicated in the figure, the weak 1A → 2A transition will be completely buried under the strong 1A → 1B absorption. Thus, the nature of the prepared state would be independent of wavelength. With virtually no variation in the relative population of 2A and 1B states at different wavelengths, the photochemistry of pro D_3 would be wavelength independent.

Acknowledgment. In Berkeley, this research was supported by PHS Grant 00709 from the National Institute of Diabetes and Digestive and Kidney Diseases. In Riverside, this research was supported by grants from the National Science Foundation (CHE8803916) and the National Institutes of Health (EY06466).

Registry No. Pre D_3, 1173-13-3; $lumi_3$, 5226-01-7; pro D_3, 434-16-2; $tachy_3$, 17592-07-3.

Supplementary Material Available: A textual presentation of the quantum yield determinations and a table listing the wavelength dependency described in the text in the solvents 2-methyltetrahydrofuran and 2,2,4-trimethylpentane (2 pages). Ordering information is given on any current masthead page.

(36) Granville, M. F.; Holtom, G. R.; Kohler, B. E. *Proc. Natl. Acad. Sci. U.S.A.* **1980**, *77*, 31.
(37) (a) Ackerman, J. R.; Kohler, B. E. *J. Am. Chem. Soc.* **1984**, *106*, 3681. (b) Adamson, G.; Gradl, G.; Kohler, B. E. *J. Chem. Phys.* **1989**, *90*, 3038.
(38) Kohler, B. E.; Mitra, P.; West, P. *J. Chem. Phys.* **1986**, *85*, 4436.